Calculating the Temperature of Electrodes in Gas-Tungsten-Arcs†

Manabu TANAKA*, Kazushi TANAKA and Masao USHIO*****

Abstract

A mathematical model of a tungsten electrode during arc discharge, which included the physical link between the tip of electrode and the arc plasma, was constructed, and the temperature distributions of the electrode were expressed numerically. The calculated results showed good agreement with observed ones concerning the temperature gradient. Furthermore, it is suggested that the usefulness of numerical experiments with this model for theoretical analysis is high and can replace experimental measurements.

KEY WORDS: (GTA Welding) (Arc) (Electrode) (Tungsten) (Mathematical Model) (Heat Conduction Equation)

1. Introduction

The durability of a tungsten electrode is the most important factor among the defects of an arc discharge applied to plasma processing. We have carried out a study of tungsten electrode for the extent of durability. Various types of tungsten electrode containing small amounts of rare-earth-metal (REM) oxides, such as La_2O_3, Y_2O_3 and Ce_2O_3, have been developed, and experiments and field tests of these electrodes have shown good durability and stability of performance particularly at the current densities applied for the usual GTA (Gas-Tungsten-Arc) welding. In the case of 2.4 mm diameter electrode, the recommended current density is below 50 A/mm^2 compared with that of thoriated tungsten[1,2,3]. However, at higher current conditions, these electrodes suffered severe erosion[4]. It appeared that REM oxides were excessively concentrated in the narrow region near the tip and associated with the formation of vacant holes. The phenomenon was considered to be caused by the migration of REM oxides and their decomposition, and the migration appeared to be strongly related with temperature distributions of the electrodes[5]. The mechanism of formation of holes, unfortunately, is not yet clear because of the difficulty of experimental measurements due to the opaque nature of an electrode veiled by high temperature plasma.

It can be deduced that numerical calculations on a model are very useful for phenomenological analysis instead of experimental measurements. Both S. Kou[6] and B.A. Dav'yanov[7] constructed mathematical models of the stationary distribution of temperature along the length of a tungsten electrode in GTA welding. Their models were based on finite-difference approximations of a stationary uni-dimensional equation for heat conduction. However, they did not suitably represent the mathematical model of a tungsten electrode during arc discharge because of a lack of physical link between the tip of electrode and the arc plasma due to a fixed temperature of the tip.

In this paper, we construct a mathematical model of a tungsten electrode during arc discharge, including the physical link between the tip of the electrode and the arc plasma, and numerically express the temperature distributions of the electrode. Furthermore, we suggest that the usefulness of numerical experiments with our model is good for phenomenological analysis instead of experimental measurements.

2. Numerical Method

2.1 Calculated region and heat conduction equation

This paper is concerned with a tungsten electrode with a flat tip as shown in **Fig. 1**. **Figure 2** shows the

† Received on 24, May, 1996
* Research Associate
** Graduate Student
*** Professor

Transactions of JWRI is published by Joining and Welding Research Institute of Osaka University, Ibaraki, Osaka 567, Japan.

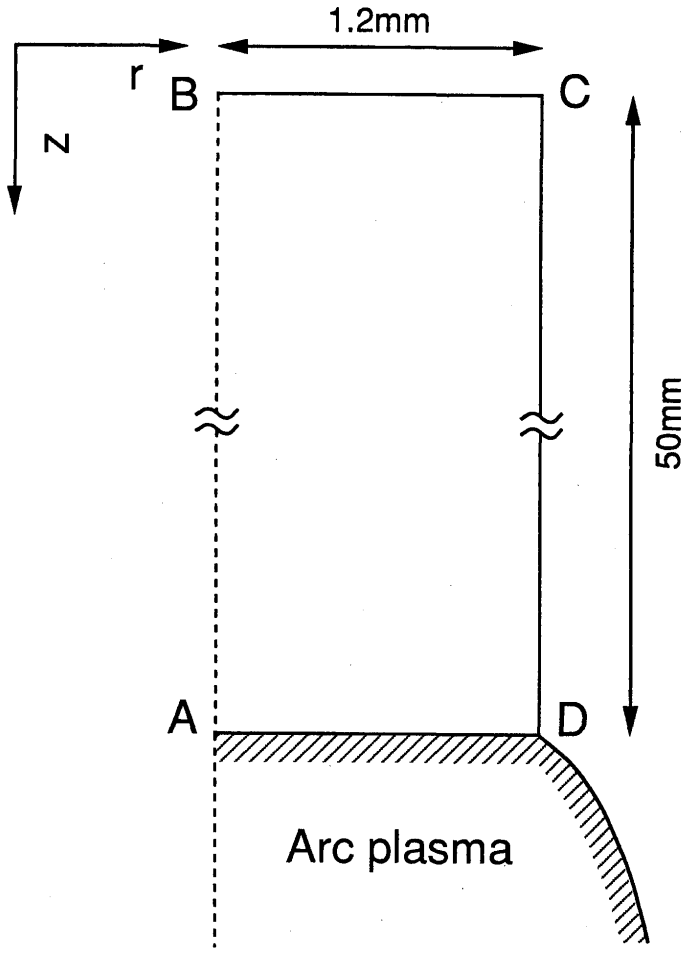

Fig. 1 Schematic illustration of the model to be solved.

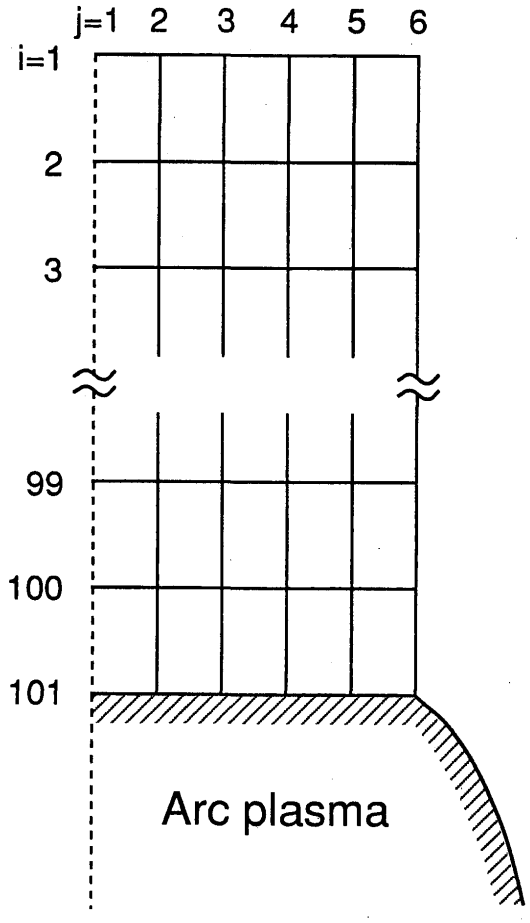

Fig. 2 Calculated region and mesh division.

calculated region and the mesh division. Since the numerical method involving finite-difference approximations of a stationary heat conduction equation have generally been used in order to calculate the temperature distributions of a solid, we used the same methods in this work.

Since some assumptions are included in our model, primary assumptions are shown as follows. Points labelled from A to D are suitable for respective alphabets in Fig. 1.

(1) Line AB is a symmetrical axis.
(2) Temperature is fixed at face BC because of cooling by water.
(3) Heat transfer into the shielding gas is taken into account at face CD.
(4) The physical link between the tip of electrode and the arc plasma is taken into account at face AD.
(5) The energy generated within the unit volume of the electrode is only Joule heat.

The following equation was solved with the above assumptions.

In generally, the heat conduction equation is given by

$$c\rho\frac{\partial T}{\partial t} = k\nabla^2 T + q, \qquad (1)$$

where T is the temperature; k is the thermal conductivity; c is the specific heat; q is the energy generated in the unit volume of the electrode; ρ is the density. However, the time element of this equation should be neglected because of the assumption of stationary heat conduction, resulting in $\partial T/\partial t = 0$. Thus, equation (1) is changed into

$$\nabla^2 T + \frac{q}{k} = 0. \qquad (2)$$

The equation (2) can be also represented in the cylindrical coordinate system, such as

$$\frac{\partial^2 T}{\partial r^2} + \frac{1}{r}\frac{\partial T}{\partial r} + \frac{\partial^2 T}{\partial z^2} + \frac{q}{k} = 0, \qquad (3)$$

where q is the Joule heat generated in the unit volume of the electrode, and it is defined as

$$q = \sigma j^2, \tag{4}$$

where σ is the electric resistivity; j is the current density.

Since equation (3) is the primary equation of heat conduction in this work, the temperature distributions of the electrode can be obtained by solving this equation with boundary conditions which are explained in the next paragraph.

2.2 Boundary conditions

In accordance with the primary assumptions, boundary conditions (= B.C.) are defined as follows.

(1) B.C. 1 (at line AB)

At line AB, the second term of equation (3) is changed into

$$\lim_{r\to 0}\left(\frac{1}{r}\frac{\partial T}{\partial r}\right) = \lim_{r\to 0}\frac{\frac{\partial}{\partial r}\left(\frac{\partial T}{\partial r}\right)}{\frac{\partial}{\partial r}(r)} = \frac{\partial^2 T}{\partial r^2}. \tag{5}$$

Thus, the heat conduction equation used at this boundary should be represented, as

$$2\frac{\partial^2 T}{\partial r^2} + \frac{\partial^2 T}{\partial z^2} + Q = 0. \tag{6}$$

(2) B.C. 2 (at face BC)

The temperature of the electrode at face BC will be assumed to be fixed and denoted T_0 because of cooling by water.

$$T = T_0 \tag{7}$$

(3) B.C. 3 (at face CD)

Figure 3 shows a control volume for the heat balance at face CD. The heat balance will be assumed to be controlled by Fourier's law ($q = -k\ grad\ T$).

a) Face abcd

The output due to conduction at face abcd is given by

$$-k\frac{T_{i,j} - T_{i,j-1}}{\Delta r}\left[\Delta z \Delta\phi\left(\frac{r_{j-1} + r_j}{2}\right)\right]. \tag{8-1}$$

b) Face aehd

The output due to conduction at face aehd is given by

$$-k\frac{T_{i,j} - T_{i+1,j}}{\Delta z}\left[\frac{\Delta r}{2}\Delta\phi\left(\frac{r_{j-1} + 3r_j}{4}\right)\right]. \tag{8-2}$$

c) Face bfgc

The output due to conduction at face bfgc is given by

$$-k\frac{T_{i,j} - T_{i-1,j}}{\Delta z}\left[\frac{\Delta r}{2}\Delta\phi\left(\frac{r_{j-1} + 3r_j}{4}\right)\right]. \tag{8-3}$$

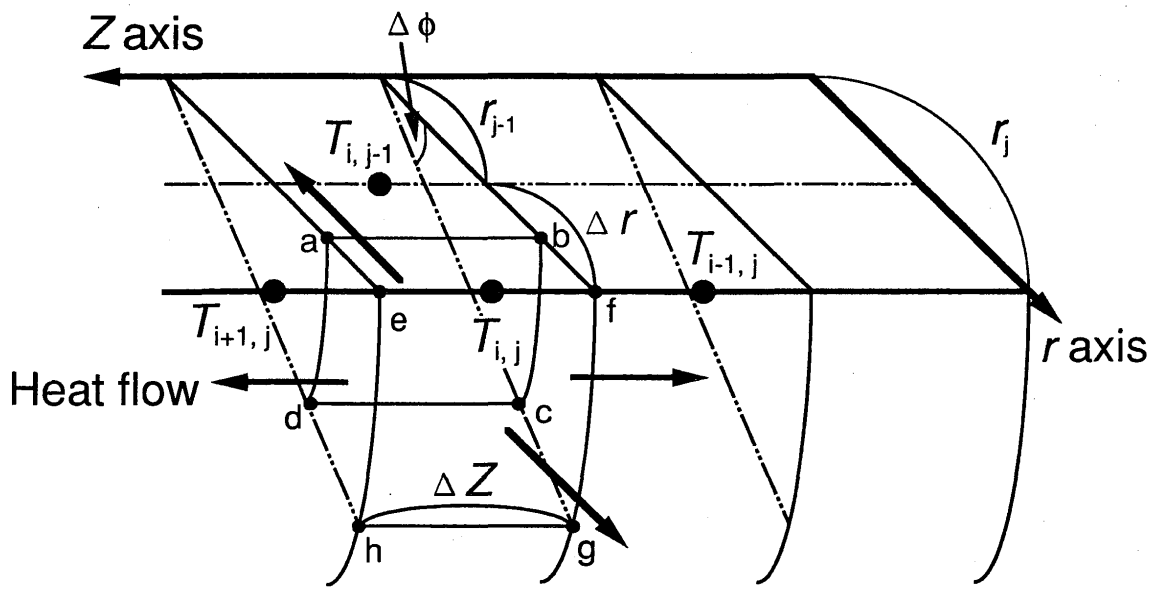

Fig. 3 Control volume for the heat balance at the electrode surface.

d) Face efgh

The output due to radiation and convection at face efgh is given by

$$-\bar{h}\left(T_{i,j}-T_G\right)\left[\Delta z\Delta\phi\cdot r_j\right] -\varepsilon\sigma_B\left(T_{i,j}-T_G\right)^4\left[\Delta z\Delta\phi\cdot r_j\right], \quad (8\text{-}4)$$

where T_G is the shielding gas temperature; $\bar{h}$ is the coefficient of convective surface heat transfer; ε is the emissivity of the electrode surface; σ_B is the Stefan-Boltzmann constant. This is based on the Stefan-Boltzmann's law and Newton's law of cooling.

e) Volume abcdefgh

The Joule heat generated in the volume abcdefgh is given by

$$q\left(\frac{\Delta r}{2}\Delta\phi\cdot r_j\cdot\Delta z\right). \quad (8\text{-}5)$$

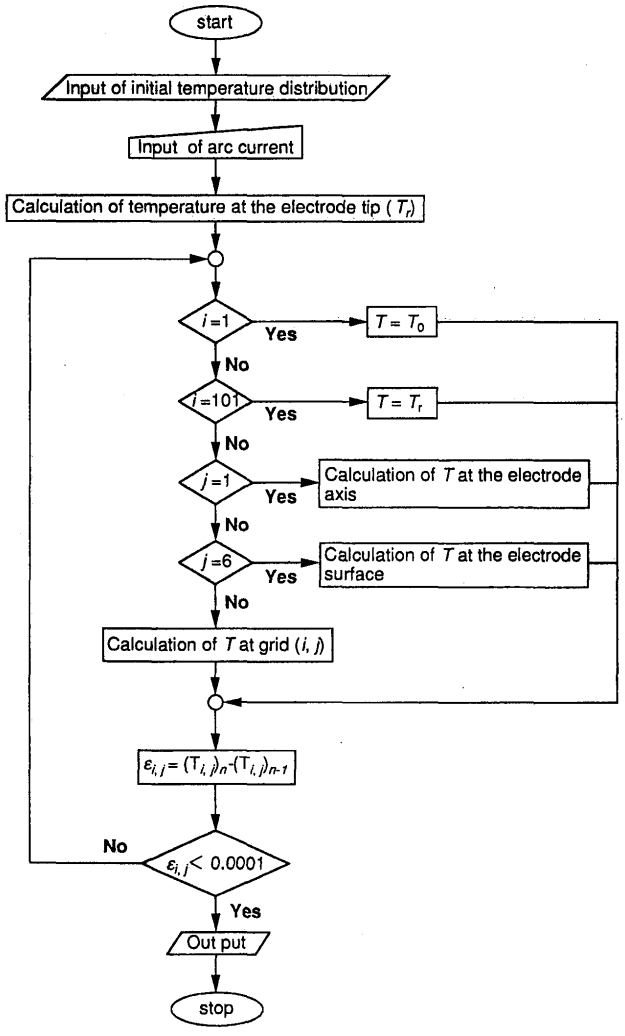

Fig. 4 Flow chart of calculation for the model.

Since the heat transfers defined by the above five equations should be balanced, the temperature of the electrode at face CD is determined by solving the equation

$$(8\text{-}1)+(8\text{-}2)+(8\text{-}3)+(8\text{-}4)+(8\text{-}5) = 0\,. \quad (9)$$

(4) B.C. 4 (at face AD)

It will be assumed that the thermoelectronic emission is satisfied at the tip of electrode (face AD) and keeps the arc discharge stable . The thermoelectronic emission is equal to the Richardson-Dushman effect which is defined by

$$J = AT^2\exp\left(-\frac{e\phi}{k_BT}\right), \quad (10)$$

where J is the current density; A is the constant depending on the material; e is the electron charge; ϕ is the work function; k_B is the Boltzmann's constant. Since the electrode diameter and arc current will be given in advance, the current density J is easily determined. If this value of J is applied to equation (10), the temperature at the tip of electrode can be determined. This numerical treatment indicates that the temperature, which is necessary to keep the arc discharge operating at a given arc current, is preserved at the tip of electrode. Thus, this

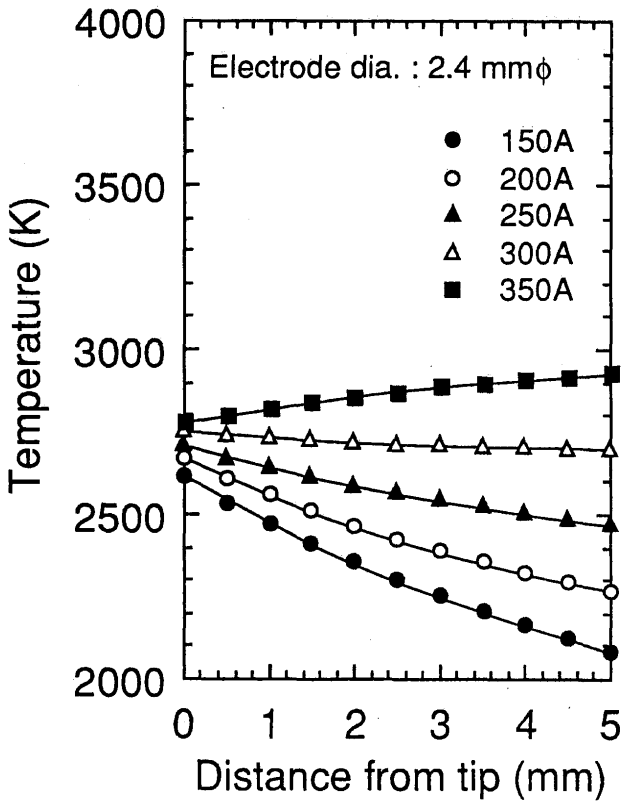

Fig. 5 Calculated temperature distributions along the electrode length.

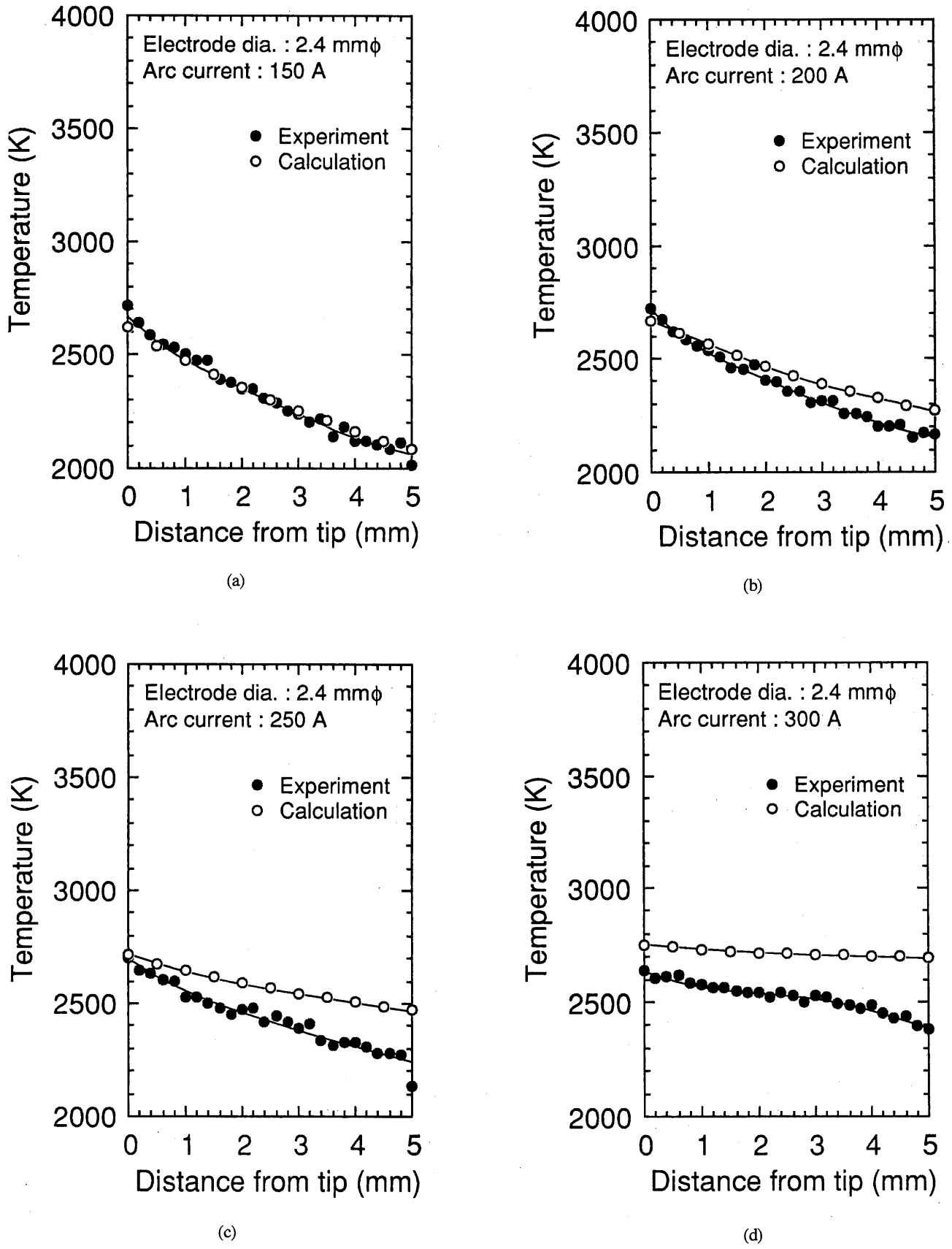

Fig. 6 Comparison between calculated and observed temperature distributions along the electrode length.
(a) 150 A (b) 200 A (c) 250 A (d) 300 A

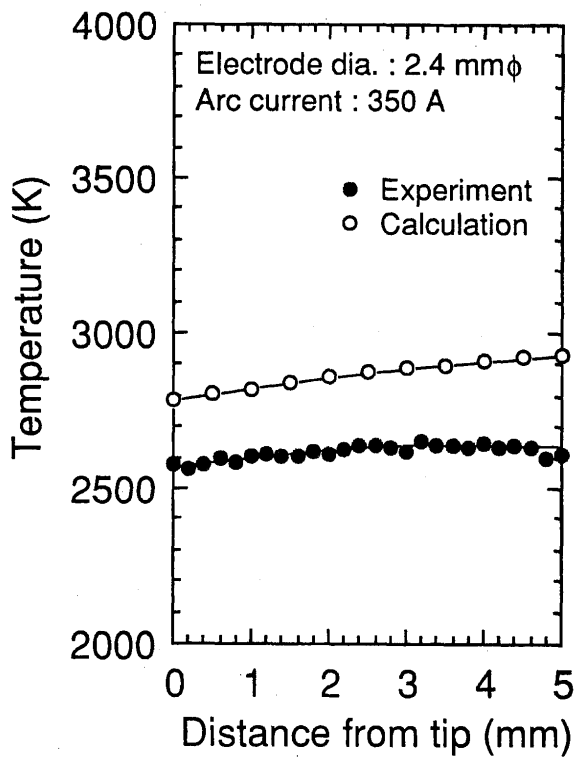

(e)

Fig. 6 Continued.
(e) 350 A

temperature will be defined by

$$T = T_r . \qquad (11)$$

2.3 Physical properties

The thermal conductivity and the electric resistivity of the electrode used in this work will be assumed to be the same as those of pure tungsten even though tungsten electrodes containing small additions were used. These properties[6] depend on temperature as follows.

Thermal conductivity : $k = 9.89T^{-0.303} \quad (J/smK)$

Electric resistivity :
$\sigma = -1.0 \times 10^{-5} + 3.333 \times 10^{-8} T \quad (\Omega \cdot m)$

Other physical properties are shown as follows.

Emissivity : $\varepsilon = 0.75$
Work function : $\phi = 2.68 \quad (eV)$
Coefficient of convective surface heat transfer :
$\bar{h} = 200 \quad (J/sm^2K^4)$
Constant of Richardson-Dushman effect : $A = 70$

In particular, the emissivity is our own experimental value and the work function employed is that of LaB_6.

2.4 Calculating procedure

Figure 4 shows the flow chart of calculation for this model. Firstly, initial temperature distribution is given by our input. Secondly, arc current is given by our input, and then the temperature at the tip of electrode is calculated. Calculation is started and repeated on the basis of the above initial conditions. If the difference between the calculated value of n times and that of n-1 times is satisfied with the convergence condition, the calculation will be stopped.

3. Results and Discussion

Figure 5 shows the calculated temperature distributions along the electrode length at the arc current of 150 A to 350 A. In the case of 150 A, the temperature immediately decreases with distance from the tip of electrode. On the other hand, in the case of 350 A, the temperature gradually increases. This suggests that the effect of Joule heat generated in the electrode immediately increases with the arc current.

Figure 6 shows the comparison between calculated and observed temperature distributions along the electrode length at the arc current of 150 A to 350 A. The observed temperature distributions of LaB_6 (0.2%)-W electrode were measured by an infrared thermal monitor produced by VANZETTI SYSTEMS INC. The experimental details concerning this measurement have been explained in earlier papers[5, 8]. In the case of low current regions, such as 150 A, the calculated temperature approximately corresponds with the observed one. However, in the case of high current regions, such as more than 250 A, the calculated temperature is about 200 K higher than the observed one. This is caused by the difference between calculated and observed temperatures at the tip of the electrode due to a lack of exactitude with regard to the heat balance at the tip. The fixed area of a cathode spot in this model must be estimated as less than the true area in the experiment with the result that the calculated temperature at the tip is higher than the observed one. However, calculated results show the good agreement with observed ones concerning the temperature gradient. Therefore, since the migration of REM oxides is strongly dependent of the temperature gradient of the electrodes, the model presented in this paper is very useful for phenomenological analysis instead of experimental measurements, although the absolute temperature of calculation slightly deviates from that of observation.

4. Conclusions

A mathematical model of a tungsten electrode during arc discharge, including the physical link between the tip

of electrode and the arc plasma, was constructed and the temperature distributions of the electrode were expressed numerically. Furthermore, it was suggested that the usefulness of numerical experiments on our model was sufficient for phenomenological analysis instead of experimental measurements.

References

1) A.A. Sadek, M. Ushio and F. Matsuda, Metallugical Trans., Vol. 21A, Dec. (1990)
2) M. Ushio and K. Tanaka, Trans. of JWRI, Vol. 22, No. 2 (1993)
3) Comm. Welding Processes of JWS, IIW Doc. XII-1047-87
4) J.M. Lafferty, J. Appl. Phys. 22 (1951), p. 299
5) M. Ushio, K. Tanaka and M. Tanaka, Trans. of JWRI, Vol. 24, No. 2 (1995)
6) S. Kou and M.C. Tsai, Welding Research Supplement, September (1985), p. 266
7) B.A. Dav'yanov, V.A. Davydov and A.V. Panyukhin, Welding International, Vol. 8, No. 9 (1994), p. 732
8) K. Tanaka, F. Matsuda and M. Ushio, Quarterly J. of the Japan Welding Society, Vol. 13, No. 4 (1995) (in Japanese)